

Uptake of Chitosan and Associated Insulin in Caco-2 Cell Monolayers: A Comparison Between Chitosan Molecules and Chitosan Nanoparticles

Zengshuan Ma¹ and Lee-Yong Lim^{1,2}

Received April 11, 2003; accepted July 9, 2003

Purpose. To evaluate the uptake of chitosan molecules (fCS) and nanoparticles (fNP), and their ability to mediate insulin transport in Caco-2 cell monolayers.

Methods. Cell-associated fCS and fNP were evaluated by fluorometry, trypan blue quenching, and confocal microscopy using FITC-labeled chitosan. Chitosan-mediated transport of FITC-labeled insulin was studied in Caco-2 cell monolayers cultured on permeable inserts.

Results. Caco-2 cells showed twofold higher association with fNP than fCS after 2-h incubation with 1 mg/ml samples. fNP uptake was a saturable (K_m 1.04 mg/ml; V_{max} 74.15 μ g/mg/h), concentration- and temperature-dependent process that was inhibited by coadministered chlorpromazine. fCS uptake was temperature dependent, but was less sensitive to concentration and was inhibited by filipin. Postuptake quenching with 100 μ g/ml of trypan blue suggests a significant amount of intracellular fNP, although the bulk of fCS was extracellular. Internalized fNP were located by confocal microscopy at 15 μ m from the apical membrane, but there was no apparent breaching of the basal membrane. This might explain the failure of the nanoparticles to mediate significant insulin transport across the Caco-2 cell monolayer.

Conclusions. Formulation of chitosan into nanoparticles transforms its extracellular interactions with the Caco-2 cells to one of cellular internalization via clathrin-mediated endocytosis.

KEY WORDS: chitosan; nanoparticles; Caco-2 cells; FITC; uptake.

INTRODUCTION

Chitosan, a polycationic polymer, is known to facilitate drug delivery across cellular barriers. Applied as a solution, the polymer enhances paracellular permeability by mediating a structural reorganization of the tight junction ZO-1 and cytoskeletal F-actin proteins (1). This action is dependent on chitosan retaining its positive charge density, which could pose a problem at physiologic pH (2). In contrast, chitosan nanoparticles were developed to transport hydrophilic macromolecules across absorptive epithelia by endocytic pathways, simultaneously protecting the drug cargo against degradation during storage and delivery (3,4). Despite the associated advantages of the nanoparticle formulation, the pharmacologic responses of an insulin-chitosan solution formulation were recently shown to be significantly larger than those produced by equivalent nanoparticle formulations in the rat and sheep models (5).

Given the potential applications of chitosan as carriers in

protein and gene delivery, a better understanding of the cellular response to chitosan presented as soluble molecules and as nanoparticles is warranted. We have previously demonstrated the feasibility of quantifying cell-associated chitosan by using stably conjugated FITC-chitosan for uptake studies in the A549 pulmonary cell model (6). Transformation of the FITC-chitosan into nanoparticles further allowed for a comparative evaluation, which showed the cellular uptake of the nanoparticles to be not only higher than that of the chitosan molecules but also unaffected by the presence of excess unlabeled chitosan molecules.

Quantification by fluorometry does not, however, discriminate between material bound to the cells extracellularly and that internalized by the cells. In many cases, the endocytosed material is confirmed by observation under a confocal microscope (7,8). However, it can be difficult to distinguish between internalized materials and those adhering to the cellular membrane, particularly for strongly bioadhesive materials. Trypan blue (TB), a dye widely used to evaluate cell viability, has been demonstrated to quench the fluorescence of FITC-labeled compounds (9,10), possibly through a change in the local pH and/or an energy transfer from the fluorophore to TB (10). Because TB is excluded by viable cells, it should be capable of quenching the fluorescence of only extracellular material, provided the material under study is not significantly cytotoxic. This technique was explored in the present study, in which postuptake incubation of the cells with TB followed by observation under a confocal microscope was used to differentiate between intracellular and extracellular chitosan.

The objective of this study was to evaluate the response of Caco-2 cells to chitosan molecules and chitosan nanoparticles and to relate this to the capacity of the chitosan formulations to mediate insulin transport across cell monolayers. The Caco-2 cells were chosen because they spontaneously differentiate into monolayers of polarized cells that resemble intestinal enterocytes when cultured on permeable inserts (11,12). Chitosan was conjugated to FITC and transformed into nanoparticles for the uptake experiments, which were carried out under various inhibiting conditions to elucidate the kinetics and mechanisms of uptake. Chitosan-mediated modification of the intercellular tight junction was evaluated by transepithelial electrical resistance measurement of the Caco-2 cell monolayers. Transport studies were conducted using commercial FITC-insulin and chitosan-insulin formulations prepared at pH 5.3 and 6.1. A previous study has shown that pH significantly modulates insulin interaction with the chitosan, resulting in nanoparticles of different properties at pH 5.3 and 6.1 (13).

MATERIALS AND METHODS

Materials

Chitosan (M_w $1.86 \pm 0.16 \times 10^5$; degree of deacetylation $84.71 \pm 0.16\%$) was purchased from Aldrich Chemical Co. (Milwaukee, WI); tripolyphosphate sodium (TPP) was from Merck (Darmstadt, Germany); minimum essential medium (MEM), fetal calf serum (FCS), nonessential amino acids (NEAA), phosphate-buffered saline (PBS, containing 8g of NaCl, 0.2g of KCl, 1.44g of Na_2HPO_4 and 0.24g of KH_2PO_4 in

¹ Department of Pharmacy, National University of Singapore, 18 Science Drive 4, Singapore 117543.

² To whom correspondence should be addressed. (email: phalimly@nus.edu.sg)

1 L), and trypsin/EDTA solution (0.2% of EDTA and 0.25% of trypsin in PBS) were from Gibco-BRL Life Technologies (Grand Island, NY); fluorescein isothiocyanate (FITC), FITC-labeled insulin (0.9 mole of FITC in 1 mol of insulin), acetic acid, methanol, Hanks' balanced salt solution (HBSS), 2-[N-morpholino] ethanesulfonic acid (MES), N-(2-hydroxyethyl)piperazine-N-(2-ethanesulfonic acid) (HEPES), benzylpenicillin, streptomycin sulfate, paraformaldehyde, trypan blue (TB), chlorpromazine, and filipin were from the Sigma Chemical Co. (St. Louis, MO); and sodium dodecyl sulfate (SDS) was from the BDH Chemicals Ltd. (Poole, England). All other chemicals were of the highest grade available commercially. Ultrapure water (Millipore, Bedford, MA) was used.

Caco-2 cells (passage 18, American Type Culture Collection, Rockville, MD) were cultured in MEM supplemented with 1% of NEAA, 10% of FCS, 100 U/ml of benzylpenicillin, and 100 µg/ml of streptomycin at 37°C in 95% air/5% CO₂ and 95% RH in a CO₂ incubator (NuAire, Plymouth, MN).

Preparation and Characterization of FITC-Labeled Chitosan Nanoparticles

Synthesis of FITC-labeled chitosan was based on the reaction between the isothiocyanate group of FITC and the primary amino group of chitosan (14). Briefly, 100 mg of FITC in 150 ml of dehydrated methanol were added to 100 ml of 1% chitosan in 0.1 M CH₃COOH. After 3 h of reaction in the dark at ambient conditions, the FITC-labeled chitosan (fCS) was precipitated by raising the pH to 8–9 with 0.5 M NaOH. To remove unconjugated FITC, the precipitate was subjected to repeated cycles of washing and centrifugation (40,000 g for 10 min) until no fluorescence was detected in the supernatant (Perkin-Elmer LS-5B spectrometer, Beaconsfield, Buckinghamshire, U.K., λ_{exc} 490 nm, λ_{emi} 520 nm). The fCS dissolved in 80 ml of 0.1 M CH₃COOH was then dialyzed for 3 days in the dark against 5 L of distilled water, the water replaced on a daily basis, before freeze drying (Dynavac Engineering, Auckland, New Zealand). The fluorescein thiocarbonyl content in the fCS was determined by fluorescence measurements against FITC standard solutions and was found to be 7.5 ± 0.53 µg/mg, equivalent to a FITC:aminoglycoside ratio of 1:290.

FITC-labeled chitosan nanoparticles (fNP) were prepared (13) by adding 4 ml of TPP solution (0.1% w/v in 0.05M NaOH) to 8 ml of fCS solution (0.2% in 0.25% CH₃COOH) at 1000 rpm (Corning Stirrer, Corning, NY) at ambient temperature. fNP dispersions were characterized and used for uptake studies immediately after preparation. Particle size and zeta potential of the nanoparticles were measured in triplicates by photon correlation spectroscopy and laser Doppler anemometry, respectively, using a particle size analyzer (Zetasizer 3000, Malvern Instruments Ltd, Worcestershire, U.K.).

Uptake Studies

Test samples consisted of stock fCS solution (2 mg/ml in 0.25% CH₃COOH) and fNP dispersion serially diluted with the uptake medium (HBSS buffered to pH 5.5 with 25 mM MES) to give chitosan concentrations of 0.27 to 1 mg/ml. Caco-2 cells (passage 48–52) cultured for 21 days on 12-well

polycarbonate plates (Nunc™, Nalge Nunc International, Denmark) at a seeding density of 1 × 10⁵ cells/cm² were washed twice with pre-warmed uptake medium and equilibrated for 30 min with 1.0 ml of the medium at 37°C. After the uptake medium was aspirated, the cells were incubated with 0.5 ml of test samples for up to 2 h at 37°C. The experiments were terminated by removing the test samples and washing the cells three times with ice-cold uptake medium. The cell lysate, obtained by solubilizing the cells/well with 1 ml of 0.1M NaOH/5% SDS, were measured for fluorescence and protein content using the plate reader (Spectra Fluor, Tecan Group Ltd., Männedorf, Switzerland; λ_{exc} 492 nm, λ_{emi} 535 nm) and protein assay kit (Micro BCA™, Pierce Chemical Company, Rockford, IL), respectively. The plate reader was calibrated with fNP and fCS samples containing chitosan concentrations of 3.47 to 27.78 µg/ml in a cell lysate solution (Caco-2 cells cultured for 21 days on 12-well plates and solubilized in 0.1 M NaOH/5% SDS at the concentration of 1 × 10⁶ cells/ml). Uptake of fNP and fCS was expressed as the amount of chitosan associated with 1 mg of cellular protein (mean ± SD, n = 3).

Parallel uptake experiments were performed at 4°C in which the Caco-2 cells were equilibrated with ice-cold uptake medium before incubation with cold fNP and fCS samples at 4°C. Uptake experiments were also conducted at 37°C in the presence of coadministered chlorpromazine (10 and 6 µg/ml) and filipin (1 µg/ml). The cells were preincubated with the uptake medium containing the specified agent, and subsequent uptake experiments were conducted in the presence of the agent.

Confocal Microscopy

To evaluate the effect of trypan blue (TB), triplicate fNP and fCS samples (100 µL, chitosan concentrations of 0.33 to 1 mg/ml) were separately incubated with 50 µL of TB solution (0 to 300 µg/ml in 0.1 M citrate buffer, pH 4.4) for 1 min in a 96-well plate at ambient conditions. The fluorescence of each sample was measured and expressed as a percentage of the fluorescence of the respective control sample (without reaction with TB).

Caco-2 cells of passage 50 were seeded at a density of 1 × 10⁵ cells/cm² onto Lab-Tek® chambered coverglass (Nalge Nunc International, Naperville, IL) and cultured for 21 days in 0.2 ml of supplemented MEM in the incubator. Medium was exchanged on alternate days. The cells, after washing twice with prewarmed uptake medium, were equilibrated with 0.1 ml of the medium for 30 min at 37°C. Uptake was initiated by adding 0.1 ml of the fNP or fCS sample to the medium to give equivalent chitosan concentration of 0.67 mg/ml. After 2 h of incubation at 37°C, the test samples were aspirated, and the cells incubated for 1 min with 0.2 ml of TB solution (100 µg/ml in 0.1 M citrate buffer, pH 4.4). The cells were then washed twice with prewarmed PBS solution before they were fixed in 3.7% paraformaldehyde and stained with propidium iodide (2 µg/ml in PBS). Cells were examined under an inverted confocal microscope (Zeiss Axiovert 200M with LSM 5 Image Browser, Carl Zeiss, Oberkochen, Germany) after storage overnight at 4°C in Jung® tissue-freezing medium (Leica Instruments, Germany).

Insulin Transport and Uptake Studies

Chitosan nanoparticles loaded with insulin were prepared (13) by premixing 1 ml of FITC-labeled insulin (2 mg/ml in 0.01M HCl) with 4 ml of 0.1% TPP before adding to 8 ml of chitosan solution (0.2% in 0.25% CH₃COOH) at 1000 rpm under ambient conditions. Nanoparticle dispersions with final pH of 5.3 and 6.1, denoted as F5.3np and F6.1np, were obtained by dissolving the TPP in 0.05 and 0.075 M NaOH, respectively. Both formulations contained a final chitosan concentration of 1.23 mg/ml. The insulin concentration was 0.154 mg/ml, of which 38.5 ± 1.5% and 78.5 ± 2.3% were associated with the nanoparticles in the F5.3np and F6.1np, respectively (13).

Control samples at pH 5.3 and 6.1 were also prepared using similar procedures except for the omission of various components from the formulation. These samples were the fI solutions (chitosan and TPP omitted); CS-fI solutions (TPP omitted); and a mixture of blank chitosan nanoparticles and insulin (denoted as NP-fI). To obtain the NP-fI samples, blank chitosan nanoparticles were first prepared by agitating the chitosan and TPP solutions together before the addition of the FITC-insulin solution (1 ml). For each experiment, the transport medium consisted of HBSS adjusted with MES to a pH corresponding to that of the samples under evaluation.

Caco-2 cells of passage 48–52 were seeded onto transwell polycarbonate cell culture inserts (12 mm diameter, 3.0 μm pore size, Costar®, Corning Incorporated, Corning, NY) at a density of 1 × 10⁵ cells/cm² and cultured for 21 days. The integrity of the Caco-2 cell monolayer was evaluated by trans-epithelial electrical resistance (TEER) measurements (Milli-cell-ERS, Millipore, Bedford, MA). To initiate the transport experiments, the culture media in the apical and basal chambers were aspirated, and the cells rinsed twice with pre-warmed transport medium. Monolayers that maintained TEER values in the range of 700–800 Ω·cm² (after deducting for blank) following a 30-min equilibration with the medium (apical 0.5 ml; basal 1.5 ml) at 37°C were used for subsequent transport experiments. The transport medium in the apical chamber was aspirated, and the cells incubated for 4 h with 0.5 ml of test or control samples at 37°C. Aliquots of 0.1 ml were withdrawn from the basal chambers and measured for fluorescence using the plate reader to determine the amounts of insulin transported. The cell monolayers after TEER measurements were also washed three times with ice-cold PBS and digested with 1 ml of 0.1 M NaOH/5% SDS. The fluorescence and protein content of the resultant cell lysates were determined using the plate reader and protein assay kit, respectively, to measure the amounts of cell-associated insulin (insulin uptake). The plate reader was calibrated with standard solutions of fI (0.52 to 4.20 μg/ml) in a cell lysate solution (1 × 10⁷ Caco-2 cells digested with 12 ml of 0.1 M NaOH/5% SDS).

Statistical Analysis

Results are expressed as means ± standard deviation. Uptake data were analyzed by one-way ANOVA followed by *post-hoc* Tukey's tests applied for comparisons of group means (SPSS 10, SPSS Inc., Chicago, IL) at a *p* value of 0.05.

RESULTS

Physical Characteristics

Table I shows the mean size, polydispersity, and zeta potential of the nanoparticle samples used in this study. The mean size of the samples remained within a relatively narrow range of 418 to 531 nm although the NP-fI (pH 6.1) sample was significantly larger than the other samples. The F6.1np and NP-fI (pH 6.1), which were both formulated at a higher pH of 6.1, also showed significantly lower zeta potential.

Uptake of fNP and fCS by Caco-2 Cell Monolayers

Uptake of fNP and fCS by the Caco-2 cell monolayers at 37°C was triphasic with respect to incubation time at all the loading concentrations studied (Fig. 1). Rapid uptake was observed in the first 30 min of contact, followed by a period of inactivity in the next 30 min, then a period of increased cellular uptake in the subsequent 1 h. Linear regression analysis yielded correlation values of >0.93 for the first 90 min and >0.91 for the entire 2-h uptake.

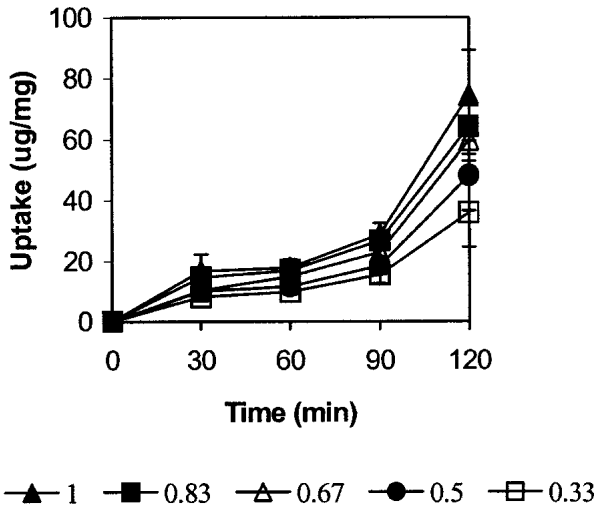
Uptake of fNP was concentration dependent, the 2-h uptake increasing by 2.07-fold, from 35.99 to 74.36 μg/mg, when the loading concentration was increased from 0.33 to 1.00 mg/ml (Fig. 1a). The process appeared to be saturable at high loading concentration (Fig. 2), and there was a good fit when the 2-h uptake data were transformed to the Michaelis-Menten equation ($R^2 = 0.996$) (Fig. 3). The K_m and V_{max} values were 1.04 mg/ml and 74.15 μg/mg/h, respectively. In contrast, the uptake of fCS by the Caco-2 cell monolayers was relatively independent of the loading concentration, although there was an increase in the 2-h uptake from 27.31 to 37.97 μg/mg when the loading concentration was increased from 0.33 to 1.00 mg/ml (Fig. 1b). At each time point and loading concentration studied, the cellular uptake of fNP exceeded that of fCS, the difference increasing with the incubation time and loading concentration. There was a twofold difference in the 2-h uptake between the fNP and fCS at the loading concentration of 1 mg/ml.

Temperature had a significant effect on the cellular uptake of the fNP and fCS (Fig. 2). The 2-h uptake of the fNP at the loading concentration of 1 mg/ml was reduced by 7.6-fold, from 89.9 ± 17.5 to 11.8 ± 2 μg/mg, when the uptake temperature was lowered from 37°C to 4°C. This decrease in

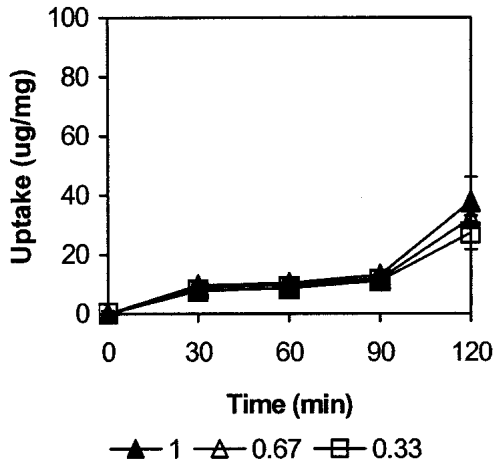
Table I. Physical Characteristics of the Nanoparticles Used in This Study

Formulation	Particle size (nm)	Polydispersity	Zeta potential (mV)
fNP	433 ± 28	0.51 ± 0.09	+27.2 ± 0.8
F5.3np	418 ± 31	0.52 ± 0.06	+29.4 ± 0.8
F6.1np	504 ± 37	0.62 ± 0.09	+14.9 ± 0.6
NP-fI (pH 5.3)	447 ± 22	0.44 ± 0.07	+28.3 ± 0.9
NP-fI (pH 6.1)	531 ± 54	0.60 ± 0.10	+13.6 ± 0.8

fNP, blank nanoparticles prepared with FITC-labeled chitosan; F5.3np and F6.1np, chitosan nanoparticles loaded with FITC-labeled insulin at pH 5.3 and 6.1, respectively; NP-fI (pH 5.3) and NP-fI (pH 6.1), blank chitosan nanoparticles mixed with FITC-labeled insulin solution at pH 5.3 and 6.1, respectively. Data represent mean ± SD, *n* = 3.



(a)



(b)

Fig. 1. Effect of loading concentration (mg/ml) on the uptake of (a) fNP and (b) fCS by Caco-2 cell monolayers at 37°C (mean ± SD, n = 6).

temperature also reduced the 2-h uptake of fCS by a similar ratio, 7.4-fold, from 45.7 ± 7.7 to 6.2 ± 0.9 µg/mg. Temperature affected the fNP and fCS uptake at all the loading concentrations studied (Fig. 2).

The cellular uptake of fNP was not affected by the presence of 1 µg/ml of filipin ($p = 0.22$), but it was significantly inhibited by coadministered chlorpromazine (Fig. 4). Cell-associated fNP was found to decrease by 32.1% and 43.8%, respectively, in the presence of 6 and 10 µg/ml of chlorpromazine. In contrast, the cellular uptake of fCS was inhibited to a greater extent by coadministered filipin than by the addition of 10 µg/ml of chlorpromazine (43.6% vs. 17.1% reduction in cell-associated fCS).

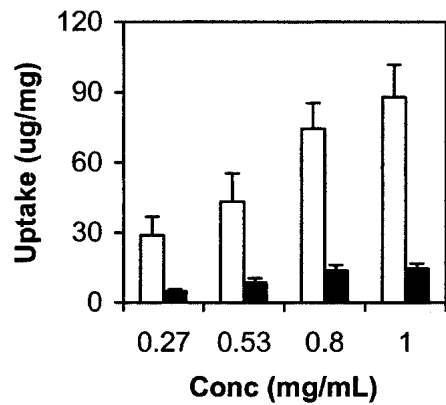
Confocal Microscopy

Incubation of fCS and fNP for 1 min with TB significantly lowered their fluorescence, with effective quenching

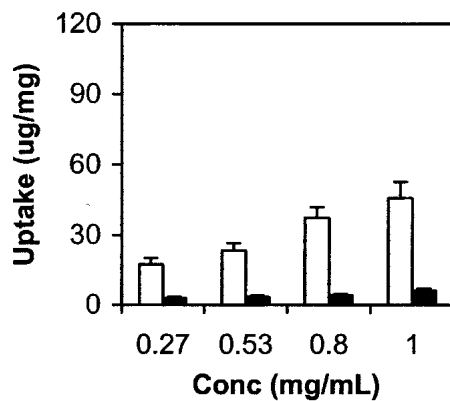
attained at a TB concentration of 33 µg/ml (100 ml of sample coincubated with 50 ml of 100 µg/ml of TB) for both samples. Subsequent experiments involving cells used a higher TB concentration of 100 µg/ml for quenching. This TB concentration is still 20 times lower than that normally used for the determination of cell viability (15).

Confluent Caco-2 cells coincubated for 2 h with 0.67 mg/ml of fNP or fCS showed strong fluorescence signals (Fig. 5A1,B1). Subsequent incubation of the Caco-2 cells for 1 min with 100 µg/ml of TB significantly reduced the fluorescence intensity (Fig. 5A2,B2). However, although those cells preincubated with fNP continued to show large areas of strong fluorescence (Fig. 5A2), only small isolated loci of fluorescence were located in the cells preincubated with fCS (Fig. 5B2). This suggests that the TB molecules were more effective at quenching the fluorescence of cell-associated fCS than fNP. Because the TB molecules were excluded by viable cells, the residual fluorescence in Fig. 5A2 implied the existence of a substantial amount of intracellular fNP.

Figure 6 shows a montage of 38 optical sections of a Caco-2 cell monolayer that had been incubated with fNP for 2 h followed by incubation with TB for 1 min. The depth of a



(a)



(b)

Fig. 2. Effect of temperature (□, 37°C; ■, 4°C) and loading concentration on the 2-h uptake of (a) fNP and (b) fCS by Caco-2 cell monolayers (mean ± SD, n = 6).

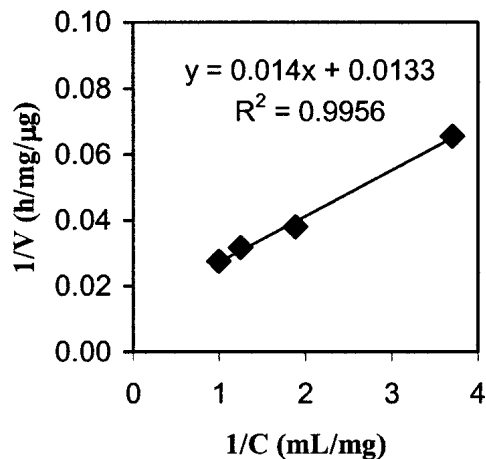


Fig. 3. Michaelis-Menten plot for fNP. Uptake was performed at 37°C for 2 h.

monolayer of Caco-2 cells was typically 20 μm . Intense fluorescence signals were concentrated between 3 and 12 μm from the apical surface of the cell monolayer, the fluorescence intensity becoming weaker at levels deeper than 12 μm and was almost absent at depths $\geq 15.75 \mu\text{m}$.

Insulin Transport and Uptake Experiments

The Caco-2 cells did not exhibit a significant increase in TEER ($p = 0.32$) after 30 min of incubation with the FITC-insulin sample at pH 5.3 (Fig. 7). In contrast, chitosan at 1.23 mg/ml significantly lowered the TEER of the Caco-2 cell monolayers at pH 5.3 (Fig. 7). Soluble chitosan appeared to exert a stronger influence, the TEER value decreasing to 17.8% and 38.8% of baseline value after 4 h of incubation with the CS-fl and NP-fl samples, respectively. The NP-fl and F5.3np samples showed similar effects on the TEER ($p = 0.12$), implicating the chitosan nanoparticles as the agent re-

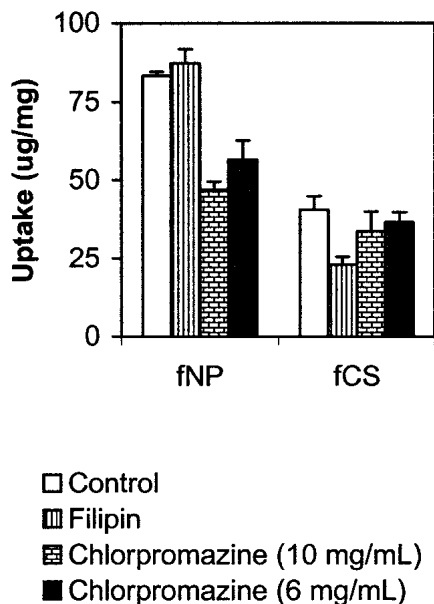


Fig. 4. Effect of chlorpromazine and filipin on the 2-h uptake of fNP and fCS by Caco-2 cell monolayers at 37°C. Loading concentration of fNP and fCS was 1 mg/ml (mean \pm SD, $n = 6$).

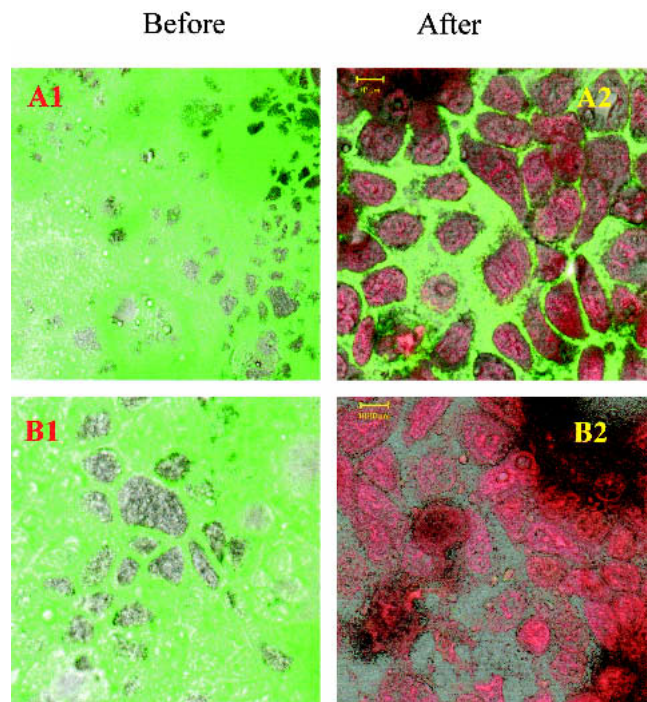


Fig. 5. Confocal micrographs of Caco-2 cell monolayers coincubated for 2 h with fNP (A) and fCS (B) before or after incubation with 100 $\mu\text{g/ml}$ of trypan blue solution.

sponsible for modulating the cellular tight junction integrity. Parallel trends were observed when the experiments were conducted at a higher pH of 6.1. At both pH values, the chitosan-mediated changes in TEER occurred within the first 30 min of incubation, similar to that reported by Kotéz *et al.* (16).

No measurable level of fluorescence was detected in the receiver chambers when the Caco-2 cells were incubated with the fl, CS-fl, NP-fl, F5.3np, and F6.1np samples, indicating that the FITC-labeled insulin was not translocated across the cell monolayers into the basal chambers after 4 h. Control experiments showed the insulin to diffuse without difficulty across the transwell insert in the absence of a Caco-2 cell monolayer. When the cell monolayers were solubilized after incubation with the samples, significant fluorescence signals indicating cell-associated insulin were detected, especially for monolayers incubated in the presence of chitosan (Fig. 8). Only 5% of the insulin in the fl sample was associated with the cells at pH 5.3, but insulin uptake was increased by 4.23 and 2.72 folds, respectively, upon the addition of soluble chitosan and chitosan nanoparticles. Interestingly, there was no difference in uptake between insulin physically mixed with the chitosan nanoparticles (NP-fl) and that incorporated into the chitosan nanoparticles during manufacture (F5.3np). Neither was there any significant difference in the uptake of insulin from a formulation when the pH was changed from 5.3 to 6.1.

DISCUSSION

Uptake of fNP by the Caco-2 cell monolayers was dependent on time, temperature and loading concentration. It was a saturable event with K_m and V_{max} values of 1.04 mg/ml and 74.15 $\mu\text{g/mg/h}$, respectively. A significant proportion of

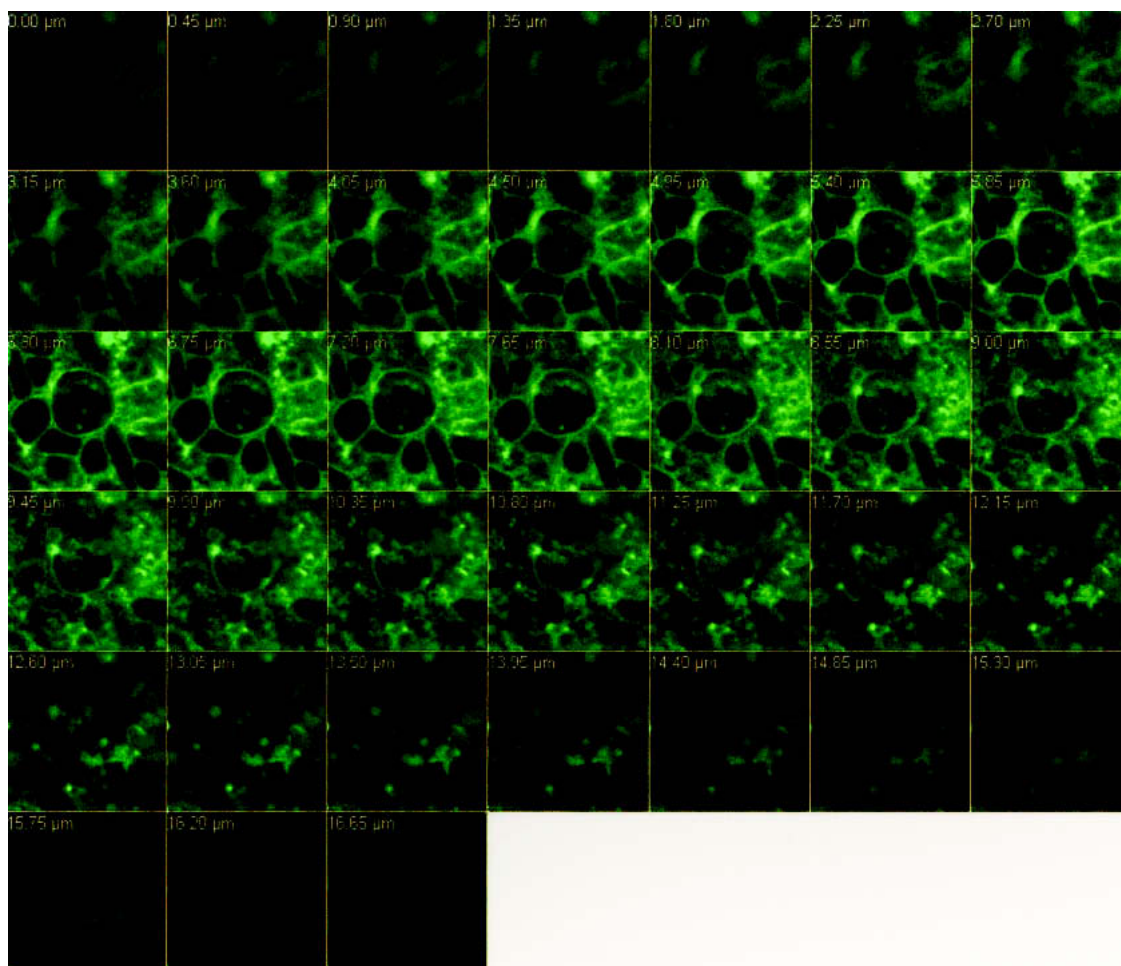


Fig. 6. Montage of confocal microscope images of Caco-2 cell monolayer incubated with 0.67 mg/ml of fNP for 2 h followed with 100 µg/ml trypan blue solution for 1 min. Optical sections were taken at intervals of 0.45 µm.

the cell-associated fNP was located within the cells. This internalization of the nanoparticles could not be attributed to a disruption of the cellular plasma membrane because the fNP did not contribute to significant changes in cell viability as assessed by TB exclusion. More likely, the fNP were internalized by the Caco-2 cells by adsorptive endocytosis, an energy-dependent, saturable process that is preceded by non-specific interaction of the cargo with the cell membrane. Chitosan is known to interact with cell membranes by electrostatic forces of attraction (1). The triphasic uptake profile suggests the possibility of a lag phase between the initial adsorption and subsequent internalization of the fNP by the Caco-2 cells.

Among the proteins identified to regulate endocytosis, clathrin, and caveolin are perhaps the most widely studied. To evaluate the role of these two proteins in the endocytosis of fNP in the Caco-2 cells, the uptake experiments were performed in the presence of chlorpromazine and filipin. Chlorpromazine at a concentration of 6 to 10 µg/ml could reduce the number of coated pit-associated receptors at the cell surface by disrupting the assembly and disassembly of clathrin (17,18). Filipin at 1 µg/ml is known to disrupt caveolae structure by binding to cholesterol and disorganizing the caveolin (19). The uptake data suggest that clathrin was important for the internalization of the fNP, its inhibition by chlorproma-

zine reducing the fNP uptake by up to 67.9%. Although clathrin-independent pathways might also be involved because the internalization of fNP was not abolished by 10 µg/ml of chlorpromazine, these pathways might not include the caveolae because the fNP uptake was unaffected by coadministered filipin.

A previous study on the uptake of fNP by a pulmonary cell line, the A549 cells, had produced similar results (6). Uptake of fNP by the A549 cells was also a concentration- and temperature-dependent, saturable process that was inhibited by coadministered chlorpromazine but not by filipin. The K_m (0.69 mg/ml) and V_{max} (58.14 µg/mg/h) values obtained for the A549 cells were also comparable. A phenomenon common to both studies is the significantly higher uptake of chitosan nanoparticles compared to chitosan molecules at equivalent loading concentrations.

Uptake of the soluble fCS by the Caco-2 cell monolayers was also a temperature dependent, triphasic event. However, the mechanism of fCS uptake appeared to be different from that of the fNP. This is because post-uptake incubation with TB effectively quenched the fluorescence of the cell-associated fCS, suggesting that the bulk of the cell-associated fCS was located extracellularly. Moreover, the fCS uptake was relatively independent of loading concentration and was more sensitive to the presence of filipin than chlorpromazine.

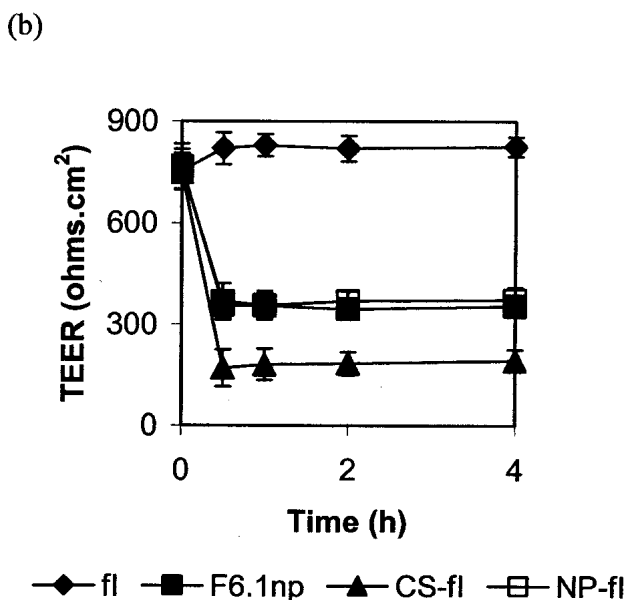
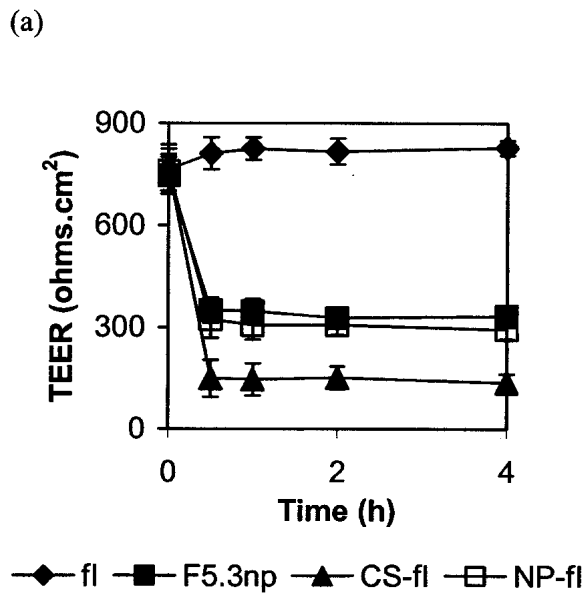


Fig. 7. Changes in the TEER ($\Omega\text{-cm}^2$) as a function of time for Caco-2 cell monolayers incubated with fl, CS-fl, NP-fl, F5.3np, and F6.1np at pH 5.3 (a) and pH 6.1 (b) (mean \pm SD, $n = 3$). fl represents solutions of FITC-labeled insulin; CS-fl represents solutions of chitosan and FITC-labeled insulin; NP-fl represents blank chitosan nanoparticles mixed with FITC-labeled insulin solution; F5.3np and F6.1np are chitosan nanoparticles loaded with FITC-labeled insulin at pH 5.3 and 6.1, respectively.

The cholesterol-binding filipin could have interfered with chitosan-membrane interaction by modifying the properties of the cell membrane (19). The present study also suggests that the soluble chitosan molecules were more effective at disrupting the intercellular tight junction than the chitosan nanoparticles, which might have interacted less effectively with the cellular proteins because of their TPP-crosslinked chitosan chains. The triphasic uptake profile of fCS implies that there was also a lag phase between the initial adsorption of the

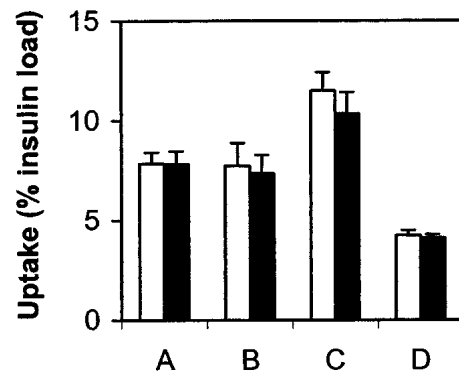


Fig. 8. Uptake of FITC-insulin by Caco-2 cell monolayers after 4 h incubation at 37°C with (A) F5.3np and F6.1np, (B) NP-fl, (C) CS-fl, and (D) fl at pH 5.3 (\square) and pH 6.1 (\blacksquare) (mean \pm SD, $n = 3$). fl represents solutions of FITC-labeled insulin; CS-fl represents solutions of chitosan and FITC-labeled insulin; NP-fl represents blank chitosan nanoparticles mixed with FITC-labeled insulin solution; F5.3np and F6.1np are chitosan nanoparticles loaded with FITC-labeled insulin at pH 5.3 and 6.1, respectively.

polymer and a subsequent uptake probably via the paracellular pathway. Interestingly, uptake of fNP at 4°C was still twice that of fCS at the loading concentration of 1 mg/ml. CS comprised of chitosan molecules with hydrodynamic size of 830 ± 516 nm while the NP were condensed particles of crosslinked chitosan molecules having average size of 433 ± 28 nm. Binding of chitosan to the cell membrane could therefore be more efficient when the polymer was presented as NP than as CS molecules.

Despite the chitosan-mediated reduction in TEER, the transport of associated insulin cargo could not be demonstrated in this study. It could be that the paracellular pathway was not adequately widened to allow for the passage of a substantial amount of insulin molecules across the cell monolayer into the basal chamber. Another reason might be the low levels of FITC-insulin in the receiver chamber, particularly for insulin transcytosed across the Caco-2 cell monolayers. Transcellular delivery of insulin via [¹²⁵I]insulin-transferrin conjugates have been demonstrated by Shah *et al.* using the Caco-2 cell model (20). The transport rate was 3 pmol/cell layer. If this transport rate was achieved in this study, insulin concentration in the basal chamber would be about 0.3 ng/ml, far below the analytic detection threshold of 100 ng/ml. Contributing to the low insulin levels might be the short incubation time and the degradation of insulin by intracellular enzymes. Confocal micrographs have shown that the fNP did not breach the basal cell membrane after 2 h of incubation.

Still, measurable amounts of insulin were found associated with the Caco-2 cells, the amount significantly enhanced by the presence of chitosan. The enhanced uptake was not correlated to the association of the insulin with the nanoparticles, for comparable data were obtained for insulin added to preformed blank chitosan nanoparticles and insulin associated with the chitosan nanoparticles during manufacture. The chitosan nanoparticles were also inferior to the soluble chitosan molecules in promoting insulin uptake by the Caco-2 cells, suggesting that the insulin uptake was facilitated through the opening of the paracellular pathway. Both phenomena parallel those reported by Dyer *et al.* (5), who observed consistently smaller pharmacologic responses in sheep

and rats administered with nasal insulin–chitosan nanoparticle formulations compared to animals given insulin–chitosan solutions. In addition, they found comparable hypoglycemic responses in rats administered with postloaded insulin–chitosan nanoparticles and insulin-loaded chitosan nanoparticles.

CONCLUSION

Transformation of chitosan into nanoparticles significantly promoted its association with the Caco-2 cell monolayers by up to 1.97-fold. It also enabled the polymer to be internalized by the cells through clathrin-dependent pathways. The uptake of chitosan nanoparticles was a concentration- and temperature-dependent, saturable event with K_m and V_{max} values of 1.04 mg/ml and 74.15 μ g/mg/h, respectively. The internalized chitosan nanoparticles were concentrated between 3 and 12 μ m from the apical surface of the cell monolayer, with no fNP detected at depths ≥ 15.75 μ m after 2 h of incubation. Although the uptake of soluble chitosan molecules was also a temperature-dependent event, it was relatively insensitive to loading concentration. The bulk of the cell-associated chitosan molecules were located extracellularly. Chitosan-mediated transcytosis of insulin could not be demonstrated, although significant amounts of insulin were associated with the Caco-2 cells. Soluble chitosan was more effective at promoting the cellular uptake of the insulin cargo, probably through its disruption of the intercellular tight junction.

ACKNOWLEDGMENTS

This study was supported by a grant (R148-000-023-112) from the National University of Singapore. Zengshuan Ma is grateful to the National University of Singapore for financial support of his graduate studies.

REFERENCES

1. N. G. Schipper, S. Olsson, J. A. Hoogstraate, A. G. deBoer, K. M. Vårum, and P. Artursson. Chitosan as absorption enhancers for poorly absorbable drugs 2: mechanisms of absorption enhancement. *Pharm. Res.* **14**:923–929 (1997).
2. A. F. Kotéz, H. L. Lueßen, A. G. deBoer, J. C. Verhoef, and H. E. Junginger. Chitosan for enhanced intestinal permeability: Prospects for derivatives soluble in neutral and basic environments. *Eur. J. Pharm. Sci.* **159**:243–253 (1997).
3. R. Fernandez-Urrusuno, P. Calvo, C. Remunan-Lopez, J. L. Vila-Jato, and M. J. Alonso. Enhancement of nasal absorption of insulin using chitosan nanoparticles. *Pharm. Res.* **16**:1576–1581 (1999).
4. H. Q. Mao, K. Roy, V. L. Troung-Le, K. A. Janes, K. Y. Lin, Y. Wang, and J. T. August. and K.W. Leong. Chitosan-DNA nanoparticles as gene carriers: synthesis, characterization and transfection efficiency. *J. Control. Rel.* **70**:399–421 (2001).
5. A. M. Dyer, M. Hinchcliffe, P. Watts, J. Castile, I. Jabbal-Gill, R. Nankervis, A. Smith, and L. Illum. Nasal delivery of insulin using novel chitosan based formulations: a comparative study in two animal models between simple chitosan formulations and chitosan nanoparticles. *Pharm. Res.* **19**:998–1008 (2002).
6. M. Huang, Z. Ma, E. Khor, and L. Y. Lim. Uptake of FITC-chitosan nanoparticles by A549 cells. *Pharm. Res.* **19**:1486–1492 (2002).
7. S. McClean, E. Prosser, E. Meehan, D. O'Malley, N. Clarke, Z. Ramtoola, and D. Brayden. Binding and uptake of biodegradable poly-DL-lactide micro- and nanoparticles in intestinal epithelia. *Eur. J. Pharm. Sci.* **6**:153–163 (1998).
8. I. Behrens, A. I. Pena, M. J. Alonso, and T. Kissel. Comparative uptake studies of bioadhesive and non-bioadhesive nanoparticles in human intestinal cell lines and rats: the effect of mucus on particle adsorption and transport. *Pharm. Res.* **19**:1185–1193 (2002).
9. C. P. Wan, C. S. Park, and B. H. S. Lau. A rapid and simple microfluorometric phagocytosis assay. *J. Immunol. Methods* **162**: 1–7 (1993).
10. S. Sahlin, J. Hed, and I. Rundquist. Differentiation between attached and ingested immune complexes by a fluorescence quenching cytofluorometric assay. *J. Immunol. Methods* **60**:115–124 (1983).
11. A. R. Hilgers, R. A. Conradi, and P. S. Burton. Caco-2 cell monolayers as a model for drug transport across the intestinal mucosa. *Pharm. Res.* **7**:902–910 (1990).
12. P. Artursson. and J. Karlsson. Correlation between oral drug absorption in humans and apparent drug permeability coefficients in human intestinal epithelial Caco-2 cells. *Biochem. Biophys. Res. Commun.* **175**:880–885 (1991).
13. Z. Ma, H. H. Yeoh, and L. Y. Lim. Formulation pH modulates the interaction of insulin with chitosan nanoparticles. *J. Pharm. Sci.* **91**:1396–1404 (2002).
14. R. B. Qaqish and M. M. Amiji. Synthesis of a fluorescent chitosan derivative and its application for the study of chitosan-mucin interactions. *Carbohydr. Polym* **38**:99–107 (1999).
15. L. Thiele, B. Rothen-Rutishauser, S. Jilek, H. Wunderli-Allenspach, and H. P. Merkle. and E. Walter Evaluation of particle uptake in human blood monocyte-derived cells *in vitro*. *J. Control. Rel.* **76**:59–71 (2001).
16. A. F. Kotéz and B. J. deLeeuw. H. L. Lueßen, A. G. deBoer, J. C. Verhoef, and H. E. Junginger. Chitosan for enhanced delivery of therapeutic peptides across intestinal epithelia: *in vitro* evaluation in Caco-2 cell monolayers. *Int. J. Pharm.* **159**:243–253 (1997).
17. P. A. Orlandi and P. H. Fishman. Filipin-dependent inhibition of cholera toxin: evidence for toxin internalization and activation through caveolae-like domains. *J. Cell Biol.* **141**:905–915 (1998).
18. A. Sofer and A. H. Futerman. Cationic amphiphilic drugs inhibit the internalization of cholera toxin to the Golgi apparatus and the subsequent elevation of cyclic AMP. *J. Biol. Chem.* **270**:12117–12122 (1995).
19. K. G. Rothberg, Y. S. Ying, B. A. Kamen, and R. G. Anderson. Cholesterol controls the clustering of the glycopospholipid-anchored membrane receptor for 5-methyltetrahydrofolate. *J. Cell Biol.* **111**:2931–2938 (1990).
20. D. Shah and W. C. Shen. Transcellular delivery of an insulin–transferrin conjugate in enterocyte-like Caco-2 cells. *J. Pharm. Sci.* **85**:1306–1311 (1996).